

Expanding the arsenal of FGFR inhibitors: a novel chloroacetamide derivative as a new irreversible agent with anti-proliferative activity against FGFR1-amplified lung cancer cell lines

Claudia Fumarola^{1*}, Nicole Bozza², Riccardo Castelli², Francesca Ferlenghi², Giuseppe Marseglia², Alessio Lodola^{2*}, Mara Bonelli¹, Silvia La Monica¹, Daniele Cretella¹, Roberta Alfieri¹, Roberta Minari⁵, Maricla Galetti⁶, Marcello Tiseo³, Andrea Ardizzoni⁴, Marco Mor², Pier Giorgio Petronini¹

¹Dipartimento di Medicina e Chirurgia, Università degli Studi di Parma, Italy,

²Department of Food and Drug Sciences, University of Parma, Italy, ³Unità di Oncologia medica, Azienda Ospedaliero-Universitaria di Parma, Italy, ⁴Oncologia Medica, Policlinico S.Orsola Malpighi, Italy, ⁵Unità di Oncologia medica, Azienda Ospedaliero-Universitaria di Parma, Italy, ⁶Dipartimento di Medicina e Chirurgia, Università degli Studi di Parma, Italy

Submitted to Journal:
Frontiers in Oncology

Specialty Section:
Cancer Molecular Targets and Therapeutics

ISSN:
2234-943X

Article type:
Original Research Article

Received on:
16 Oct 2018

Accepted on:
04 Mar 2019

Provisional PDF published on:
04 Mar 2019

Frontiers website link:
www.frontiersin.org

Citation:
Fumarola C, Bozza N, Castelli R, Ferlenghi F, Marseglia G, Lodola A, Bonelli M, La_monica S, Cretella D, Alfieri R, Minari R, Galetti M, Tiseo M, Ardizzoni A, Mor M and Petronini P(2018) Expanding the arsenal of FGFR inhibitors: a novel chloroacetamide derivative as a new irreversible agent with anti-proliferative activity against FGFR1-amplified lung cancer cell lines. *Front. Oncol.* 9:179. doi:10.3389/fonc.2019.00179

Copyright statement:
© 2019 Fumarola, Bozza, Castelli, Ferlenghi, Marseglia, Lodola, Bonelli, La_monica, Cretella, Alfieri, Minari, Galetti, Tiseo, Ardizzoni, Mor and Petronini. This is an open-access article distributed under the terms of the [Creative Commons Attribution License \(CC BY\)](https://creativecommons.org/licenses/by/4.0/). The use, distribution and reproduction in other forums is permitted, provided the original author(s) or licensor are credited and that the original publication in this journal is cited, in accordance with accepted academic practice. No use, distribution or reproduction is permitted which does not comply with these terms.

This Provisional PDF corresponds to the article as it appeared upon acceptance, after peer-review. Fully formatted PDF and full text (HTML) versions will be made available soon.

Provisional

1 **Expanding the arsenal of FGFR inhibitors: a novel chloroacetamide**
2 **derivative as a new irreversible agent with anti-proliferative activity**
3 **against FGFR1-amplified lung cancer cell lines**
4
5

6 Claudia Fumarola^{1#*}, Nicole Bozza^{2#}, Riccardo Castelli², Francesca Ferlenghi², Giuseppe
7 Marseglia², Alessio Lodola^{2*}, Mara Bonelli¹, Silvia La Monica¹, Daniele Cretella¹, Roberta Alfieri¹,
8 **Roberta Minari³, Maricla Galetti^{4,5}**, Marcello Tiseo³, Andrea Ardizzoni⁶, Marco Mor^{2§}, Pier Giorgio
9 Petronini^{1§}

10
11
12 ¹Department of Medicine and Surgery, University of Parma, Parma, Italy

13 ²Department of Food and Drug, University of Parma, Parma, Italy

14 ³Medical Oncology Unit, University Hospital of Parma, Parma, Italy

15 ⁴Italian Workers' Compensation Authority (INAIL) Research Center, Parma, Italy

16 ⁵Center of Excellence for Toxicological Research (CERT), Department of Medicine and Surgery,
17 University of Parma, Italy

18 ⁶Division of Medical Oncology, Sant'Orsola-Malpighi University Hospital and Alma Mater
19 University of Bologna, Bologna, Italy

20
21
22 * Correspondence:

23 Claudia Fumarola

24 claudia.fumarola@unipr.it

25
26 Alessio Lodola

27 alessio.lodola@unipr.it

28
29
30 #These authors contributed equally to the work

31 §Co-last authors

32
33
34 Running title: UPR1376: a new irreversible FGFR inhibitor

35
36
37 Number of words: 7,022

38 Number of figures: 7 Figures; 1 Table; 2 Supplementary Figures

51 **Abstract**

52 Fibroblast Growth Factor Receptors (FGFR1–4) have a critical role in the progression of several
53 human cancers, including Squamous Non-Small-Cell Lung Cancer (SQCLC). Both non-selective
54 and selective reversible FGFR inhibitors are under clinical investigation for the treatment of
55 patients with tumors harboring FGFR alterations. Despite their potential efficacy, the clinic
56 development of these drugs has encountered several challenges, including toxicity and the
57 appearance of drug resistance.

58 Recent efforts have been directed at development of irreversible FGFR inhibitors, which have the
59 potential to exert superior anti-proliferative activity in tumors carrying FGFR alterations. With this
60 in mind, we synthesized and investigated a set of novel inhibitors possessing a warhead potentially
61 able to covalently bind a cysteine in the P-loop of FGFR. Among them, the chloroacetamide
62 UPR1376 resulted able to irreversibly inhibit FGFR1 phosphorylation in FGFR1 over-expressing
63 cells generated from SQCLC SKMES-1 cells. In addition, this compound inhibited cell
64 proliferation in FGFR1-amplified H1581 cells with a potency higher than the reversible inhibitor
65 BGJ398 (infigratinib), while sparing FGFR1 low-expressing cells. The anti-proliferative effects of
66 UPR1376 were demonstrated in both 2D and 3D systems and were associated with the inhibition of
67 MAPK and AKT/mTOR signaling pathways. UPR1376 inhibited cell proliferation also in two
68 BGJ398-resistant cell clones generated from H1581 by chronic exposure to BGJ398, although at
69 concentrations higher than those effective in the parental cells, likely due to the persistent activation
70 of the MAPK pathway **associated to NRAS amplification**. Combined blockade of FGFR1 and
71 MAPK signaling, by UPR1376 and trametinib respectively, significantly enhanced the efficacy of
72 UPR1376, providing a means of circumventing resistance to FGFR1 inhibition. Our findings
73 suggest that the insertion of a chloroacetamide warhead on a suitable scaffold, as exemplified by
74 UPR1376, is a valuable strategy to develop a novel generation of FGFR inhibitors for the treatment
75 of SQCLC patients with FGFR alterations.

76

77 **Keywords**

78 FGFR, irreversible inhibitors, drug design, lung cancer, SQCLC, cancer drug resistance

79

80

81

82

83

84

85

86

87

88

89

90

91

92

93

94

95

96

97

98

99

100 Introduction

101 The Fibroblast Growth Factor Receptor (FGFR) tyrosine kinase (TK) family consists of four
102 members (FGFR1-4), activated through 22 different FGF ligands, which regulate multiple
103 biological processes, including cell proliferation, migration, differentiation, apoptosis, metabolism,
104 and angiogenesis (1). Upon ligand binding, FGFRs dimerize and activate a complex downstream
105 signaling, including mitogen activated protein kinase (MAPK), phosphoinositide-3-kinase
106 (PI3K)/Akt, and signal transducer and activator of transcription (STAT) pathways (2). Deregulation
107 of FGFR signaling, via gene amplification, overexpression, point mutations or chromosomal
108 translocations has been implicated in several human cancers, such as lung, breast, prostate, and
109 endometrial cancers (3). In lung cancer, FGFR1 amplification is observed in 9-20% of cases of the
110 Squamous Non-Small-Cell Lung Cancer (SQCLC) histotype (3-5). SQCLC is a challenging disease
111 characterized by a marked mutational complexity that renders difficult the development of effective
112 molecular-targeted therapies. Although immunotherapy has recently shown great promise (6-9),
113 platinum-based regimens are still the standard of care 1st-line therapy for the majority of patients.
114 Therefore, the potential of FGFR signaling as a therapeutic target in SQCLC warrants continued
115 exploration to provide a valuable treatment option at least for the subset of patients carrying FGFR
116 alterations.

117 Since the identification of FGFR as a relevant target for cancer therapy, a number of FGFR
118 inhibitors have been developed and some are currently under clinical evaluation in various FGFR-
119 related tumors (10). The most clinically advanced compounds are non-selective FGFR TKIs, such
120 as dovitinib and the Food and Drug Administration (FDA)-approved ponatinib, which target other
121 related TKs, including Vascular Endothelial Growth Factor Receptors (VEGFRs) and Platelet
122 Derived Growth Factor Receptors (PDGFRs). Despite their potential efficacy, the clinic success of
123 these drugs is limited by the increased adverse side effects associated with their broad inhibitory
124 activity (2). More recently, potent and highly selective FGFR inhibitors, such as BGJ398
125 (infigratinib, Figure 1) and others, i.e. AZD-4547 (11) and JNJ-42756493 (erdafitinib (12)), have
126 shown promising pre-clinical anti-tumor activity, thereby entering into clinic investigation.
127 However, although these agents display a more favorable safety profile as compared to FGFR non-
128 selective inhibitors (13, 14), their clinical efficacy has not been unequivocally demonstrated, with
129 the less encouraging results obtained in patients with FGFR1 amplification (15, 16). Moreover, as
130 seen with other RTK inhibitors, the clinical benefit of FGFR-targeted therapies is inevitably
131 hampered by the emergence of acquired resistance (17), arising from activation of by-pass signaling
132 mechanisms or selection of gatekeeper mutations that abrogate the drug inhibitory activity on the
133 receptor.

134 Inhibitors able to engage FGFR with an irreversible mechanism of action have the potential to
135 overcome the effect of genetic alterations emerging in FGFR inhibitor-treated tumors (18). The
136 clinical experience gained in the field of EGFR and BTK kinases (19) have shown that compounds
137 of this kind are more therapeutically effective than their reversible analogues, in light of the
138 following properties: *i.* irreversible inhibitors do not readily dissociate from the engaged target
139 thanks to the formation of a covalent bond; *ii.* they cannot be displaced by ATP once the covalent
140 bond with the target is formed; *iii.* they sustain prolonged inhibition of the signaling pathways also
141 after elimination from the cells, as the inhibitory process can be reverted only through the *de novo*
142 synthesis of the protein (20, 21). Recent attempts to develop irreversible inhibitors of FGFR have
143 led to the identification of acrylamide-based compounds such as FIIN-2/FIIN-3 (18) and PRN1371
144 (22) (Figure 1), which alkylate a non-catalytic cysteine present in the P-loop of FGFR isoforms
145 (Cys488 in FGFR1). These compounds show excellent anti-proliferative activity in a variety of lung
146 cancer cell lines with a potency comparable or superior to that of the clinical candidate BGJ398 (18,
147 22). These compounds also inhibited the growth of SQCLC cell lines resistant to BGJ398, emerging
148 as potentially useful for treating FGFR-dependent cancers, such as cholangiocarcinoma or
149 metastatic urothelial cancer, after progression (23). In the present work, we report and characterize
150 a focused set of FGFR inhibitors based on the 1-(4-aminobenzyl)-pyrimido[4,5-d]pyrimidin-2-one

151 core of FIIN-2, equipped with warheads different from acrylamide, with the aim to expand the
152 arsenal of available irreversible agents targeting FGFR.

153

154 **Materials and Methods**

155

156 **Cell culture**

157 The human NSCLC cell lines SKMES-1 and H1581 were purchased from the American Type
158 Culture Collection (ATCC, Manassas, VA); ATCC authenticates the phenotypes of these cell lines
159 on a regular basis. FGFR1-over-expressing LENTI-4 cells were generated from FGFR1-low-
160 expressing SKMES-1 cells using a lentiviral vector system, as previously described (24). BGJ398-
161 resistant cells were generated from H1581 cells by continuous culturing with increasing
162 concentrations of BGJ398 up to 1 μ M, and were routinely maintained in the presence of 1 μ M
163 BGJ398. All the cells were cultured in RPMI 1640 medium, supplemented with 2 mM L-glutamine,
164 10 % fetal calf serum (FCS), and 1 % penicillin/streptomycin solution, and maintained at 37°C in a
165 humidified atmosphere of 5 % CO₂ and 95 % air.

166

167 **Compounds**

168 BGJ398 was provided by Novartis International AG (Basel, Switzerland). FIIN-2 was purchased
169 from Selleck Chemicals (Houston, TX). UPR1371-76 were prepared as described in the
170 Supplementary Material. All the drugs were dissolved in DMSO (Sigma-Aldrich, Saint Louis, MO)
171 and diluted in fresh medium before use. The final concentration of DMSO in medium never
172 exceeded 0.1 % (v/v) and equal amounts of the solvent were added to control cells.

173

174 **Western blotting analysis**

175 Procedures for protein extraction, solubilization, and protein analysis by 1-D PAGE are described
176 elsewhere (25). Antibodies against p-FGFR^{Tyr653/654}, FGFR1, p-ERK1/2^{Thr202/Tyr204}, ERK1/2, p-
177 mTOR^{Ser2448}, mTOR, p-AKT^{Ser473}, AKT, p-P70S6K^{Thr389}, P70S6K were from Cell Signaling
178 Technology (Beverly, MA); the antibody against actin was from Sigma-Aldrich. HRP-conjugated
179 secondary antibodies were from Pierce (Rockford, IL) and chemiluminescence system
180 (Immobilion™ Western Chemiluminescent HRP Substrate) was from Millipore (Temecula, CA).
181 The chemiluminescent signal was acquired by C-DiGit® Blot Scanner (LI-COR Biotechnology,
182 Lincoln, NE). Where indicated, phosphorylation levels were quantified by Image Studio™ Software
183 (LI-COR Biotechnology), and normalized to the corresponding protein levels.

184

185 **Autophosphorylation and washout assay**

186 The cells, serum-starved for 24 hours, were pre-incubated for 1 hour with the compounds at 1 μ M
187 concentration and then stimulated for 15 min with 25 ng/ml FGF2 (Miltenyi Biotec, Bergisch
188 Gladbach, Germany). For the washout assay, the cells, pre-incubated with the compounds for 1
189 hour, were extensively washed with PBS, and then maintained in drug-free medium for additional 8
190 hours before stimulation with FGF2 for 15 min. The cells were lysed and equal amounts of cell
191 protein extracts were analyzed by Western blotting using a phospho-FGFR antibody. Membranes
192 were stripped and re probed with anti-FGFR1 antibody.

193

194 **Determination of intracellular concentrations of selected compounds**

195 The cells were plated at 1×10^6 cells/dish (25 cm²) density. After 24 hours, BGJ398, FIIN-2 or
196 UPR1376 were added to the culture medium (titled concentration: 1 μ M with DMSO 0.1 % v/v). At
197 the end of incubation, the compounds were removed from the extracellular medium by washing the
198 cells for three times with 1 mL aliquot of fresh medium. The cells were treated using absolute EtOH
199 (1.1 mL at 4 °C) to obtain intracellular extracts. The final cell extracts were centrifuged (4 °C,
200 10,000g, 5 min) and collected. A fixed volume of ethanolic extract was evaporated to dryness,
201 dissolved in LC eluent and injected into the LC/MS system for quantitative measurement (see

202 Supplementary Material for details). Cell proteins were quantified after solubilization in NaOH 0.5
203 N (2 mL/25 cm² dish) by the Bradford method.

204

205 **Analysis of cell proliferation**

206 Cell proliferation was evaluated by tetrazolium dye [3-(4,5-dimethylthiazol-2-yl)-2,5-
207 diphenyltetrazolium bromide (MTT), Sigma Aldrich] assay, as previously described (26). The
208 concentration that inhibits 50 % of cell proliferation (IC₅₀) was extrapolated from the dose-response
209 curves calculated from experimental points using Graph-Pad Prism version 6.0 software (GraphPad
210 Software, San Diego, CA). The nature of the interaction between UPR1376 and trametinib was
211 calculated using the Bliss additivism model (27). A theoretical dose-response curve was calculated
212 for combined inhibition using the equation of Bliss = EA + EB-EA*EB, where EA and EB are the
213 percent of inhibition versus control obtained by UPR1376 (A) and trametinib (B) alone and the E
214 Bliss is the percent of inhibition that would be expected if the combination was exactly additive. If
215 the combination effect is higher than the expected Bliss equation value, the interaction is
216 synergistic, while if the effect is lower, the interaction is antagonistic. Otherwise, the effect is
217 additive and there is no interaction between the drugs.

218

219 **Spheroid generation**

220 Spheroids were generated using LIPIDURE[®]-COAT PLATE A-U96 (NOF Corporation, Tokyo,
221 Japan) as previously described (28). Briefly, 500 cells were seeded in RPMI 1640 medium and after
222 three days (T₀) the spheroids were treated with BGJ398, FIIN-2 or UPR1376 for further 10 days.
223 The effect of the drugs was evaluated in term of volume changes using the Nikon Eclipse E400
224 Microscope with digital Net camera. The volume of spheroids was measured [$D=(D_{max}+D_{min})/2$;
225 $V=4/3\pi(D/2)^3$] using SpheroidSizer, a MATLAB-based and open-source software application (29).

226

227 **Analysis for the presence of FGFR1 p.V561M mutation**

228 Genomic DNA was extracted from the cells using the QIAamp DNA Mini Kit (Qiagen Inc.,
229 Valencia, CA, USA), and stored at -20°C until use. Primers were designed in FGFR1 exon 13 with
230 Primer3 software.

231 FGFR1-exon13 Forward 5' tgctcgggaattttctggac 3'

232 FGFR1-exon13 Reverse 5' caacgccaccacaagatgat 3'

233 Exon 13 of FGFR1 gene (GeneBank accession number NM_023110) was amplified for each
234 sample by Polymerase Chain Reaction (PCR) using AmpliTaq Gold DNA Polymerase (Applied
235 Biosystems) following manufacturer's protocol. PCR conditions were the following: 95°C for 10
236 minutes, 15 cycles with touch down protocol with annealing temperature (TA) from 63°C to 56°C
237 and 35 cycles with TA at 56°C. A final step of 10 minutes at 72°C was performed. Genomic DNA
238 was sequenced using a CEQ Dye-Terminator Cycle Sequencing kit (Beckman Coulter Inc., Miami,
239 FL, USA) according to the manufacturer's protocol. Sequence alignments were performed with the
240 DNASTar program (DNASTar Inc., Madison, WI, USA). All the sequence reactions were performed
241 using a CEQ XL2000 DNA Analysis System (Beckman Coulter).

242

243 **NRAS amplification**

244 The analysis of NRAS amplification was performed by a digital droplet PCR (ddPCR), using a Copy
245 Number Assay (BioRad®, Hercules, CA) following the manufacturer's instructions.

246 NRAS assay (dHsaCP1000493, BioRad) was labelled in FAM, and reference assay AP3B1
247 (dHsaCP2500348), chosen among recommended reference assays by BioRad, was labelled in VIC.

248

249

250 **Statistical analysis**

251 Statistical analyses were carried out using Graph-Pad Prism version 6.0 software. Statistical
252 significance of differences among data was estimated by Student's t test and p values are indicated

253 where appropriate in the figures and in their legends. p values less than 0.05 were considered
254 significant.

255

256 Results

257

258 Chemistry

259 Starting from the structure of FIIN-2 (Figure 2A), we synthesized a small set of new potential
260 FGFR inhibitors replacing the terminal acrylamide installed on the aminobenzyl pendant of this
261 compound with other chemical groups. Our design strategy was based on two distinct approaches.
262 With the first, we masked the acrylamide warhead by preparing the 3-aminopropanamide (3-APA)
263 derivative UPR1371. The 3-APA group is not itself capable to covalently bind nucleophiles, but it
264 can undergo selective activation in the intracellular environment of cancer cells, (30) releasing the
265 acrylamide group (Figure 2B). With the second, the acrylamide was replaced by activated
266 acetamides, i.e. by electrophilic groups potentially able to alkylate the P-loop cysteine of FGFR
267 isoforms by nucleophilic substitution (Figure 2C), differently from acrylamides which still alkylates
268 cysteine residues, but with a different mechanism, namely a Michael addition. This is the case of 2-
269 ((1*H*-imidazol-2-yl)thio)acetamide UPR1372, 2-((1*H*-tetrazol-5-yl)thio)acetamide UPR1373 and 2-
270 chloroacetamide UPR1376. Acetamides of this kind have been recently used by our group to obtain
271 irreversible inhibitors of EGFR (31, 32) **Castelli 2018, manuscript submitted (33)** that also
272 possesses a critical cysteine at the ATP binding site. The procedures employed to synthesize the
273 title compounds, along with their chemical characterization, are reported in the Supplementary
274 Material.

275

276 UPR1376 inhibits FGFR1 auto-phosphorylation irreversibly in FGFR1 over-expressing 277 SQCLC cells

278 The newly synthesized compounds were analyzed for their ability to inhibit FGFR auto-
279 phosphorylation in LENTI-4 cells, a FGFR1-over-expressing cell model generated in our lab from
280 SQCLC FGFR1 low-expressing SKMES-1 cells. As indicated in Figure 3, all the compounds down-
281 regulated FGF2-induced phosphorylation of FGFR1 after 1 hour of treatment, with an efficacy
282 comparable to that shown by the reversible FGFR inhibitor BGJ398 and the irreversible reference
283 inhibitor FIIN-2. To test the irreversible activity of UPR1371-UPR1376 compounds, wash-out
284 experiments were performed in which LENTI-4 cells were exposed to the drugs for 1 hour,
285 extensively washed with PBS, and then incubated in drug-free medium for further 8 hours before
286 stimulation with FGF2. While UPR1371, 1372, and 1373 failed to maintain FGFR1 inhibition,
287 allowing an almost complete recovery of auto-phosphorylation after 8 hours, UPR1376 was even
288 more effective than FIIN-2 in sustaining the inhibition of FGFR1 auto-phosphorylation (Figure 3),
289 suggesting its ability to covalently interact with the receptor. As expected, FGFR1 auto-
290 phosphorylation was reversibly inhibited by BGJ398 and recovered 8 hours after BGJ398
291 withdrawal, although the restoration was not complete, presumably because of the efficient trapping
292 of the drug into the cells (34).

293 To further characterize the biological activity of the most interesting compounds (BGJ398, FIIN-2
294 and UPR1376), we measured their intracellular level in LENTI-4 cells immediately after 1 hour of
295 exposure to **each** inhibitor (nominal concentration of 1 μ M) or 8 hours after washing the inhibitor
296 from the extracellular medium by LC/MS (see Supplementary Material for details). Measured
297 concentrations are summarized in Table 1. At both time points, the chloroacetamide derivative
298 UPR1376 displayed an intracellular concentration significantly lower than BGJ398 or FIIN-2. This
299 could be ascribed **to its lower metabolic stability, as indicated by the residual compound
300 concentration measured in the cellular medium after 8 h, i.e., 69.4 ± 2.5 % for UPR1376, 90.2 ± 9.0
301 for BGJ398, and 85.1 ± 2.8 % for FIIN-2, to a reduced ability of UPR1376 to penetrate into LENTI-
302 4 cells or to a lower chemical stability in the cellular environment or to a combination of both
303 factors.** In spite of a lower intracellular concentration, UPR1376 resulted able to inhibit FGFR auto-

304 phosphorylation as effectively as BGJ398 and FIIN-2 at 1 hour and even more than these two
305 reference compounds 8 hours after compound removal. This suggests that UPR1376 is more potent
306 than BGJ398 and FIIN-2 in the auto-phosphorylation assay.

308 **UPR1376 down-regulates FGFR1 signaling and inhibits cell proliferation in FGFR1-amplified** 309 **H1581 cells**

310 The anti-tumor activity of UPR1371-UPR1376 was then evaluated in the NSCLC large cell
311 carcinoma H1581 cell line, a cell model that harbors focal amplification of FGFR1 and is
312 exquisitely sensitive to FGFR1 inhibition. All the compounds significantly inhibited cell
313 proliferation with IC₅₀ values in the nM range (Figure 4A). However, UPR1371 was the least
314 effective, showing an IC₅₀ value of ~55 nM; UPR1376 again demonstrated high efficacy, inhibiting
315 cell proliferation with an IC₅₀ value lower than that obtained with BGJ398 treatment. These growth-
316 inhibitory effects were associated with the inhibition of FGFR1 phosphorylation, with consequent
317 down-regulation of downstream signaling (Figure 4B). In particular, all the compounds were as
318 effective as BGJ398 and FIIN-2 in inhibiting the MAPK pathway, as indicated by the complete
319 dephosphorylation of ERK1/2 proteins, whereas the AKT pathway, with its downstream
320 components mTOR and p70S6K, was more strongly down-regulated by UPR1376. Since UPR1376
321 appeared more effective than BGJ398 in two dimensional (2D) cultures, we evaluated its anti-
322 proliferative activity also in three dimensional (3D) systems. As shown in Figure 4C, we
323 demonstrated that not only BGJ398 and FIIN-2, but also UPR1376 completely inhibited the growth
324 of tumor spheroids generated from H1581 cells, confirming its efficacy as an inhibitor of FGFR1-
325 dependent cell growth.

327 **Generation and characterization of BGJ398-resistant H1581-derived cell clones**

328 **UPR1376 inhibits cell growth in BGJ398-resistant H1581-derived cell clones and this effect is** 329 **enhanced by the combination with the MEK1/2 inhibitor trametinib**

330 The efficacy of the newly synthesized compounds was also evaluated in BGJ398-resistant cell
331 clones generated from H1581 cells. Continuous exposure of H1581 cells to 50 nM BGJ398 initially
332 led to **the** inhibition of cell proliferation associated with cell death. During culture, the concentration
333 of BGJ398 was gradually increased up to 1 μM, and after 3 months of continuous treatment the
334 selective pressure finally led to the emergence of cells no longer sensitive to the drug. Two
335 independent cell clones were selected (H1581R1 and H1581R2), which, in contrast with the
336 parental cell line, could grow in the presence of 1 μM BGJ398 and showed an IC₅₀ value for cell
337 proliferation > 4 μM (Figure 5A). As shown in Figure 5B, resistance of these cell clones to BGJ398
338 was associated with a persistent phosphorylation of FGFR1 despite the presence of BGJ398, in
339 contrast with the almost complete inhibition induced by the drug in sensitive H1581 parental cells.

340 **We therefore performed Sanger sequencing of PCR products from H1581R cell clones to evaluate**
341 **whether the resistance to FGFR1 inhibition was due to the presence of the V561M mutation at the**
342 **gatekeeper residue located in the ATP-binding pocket of the receptor (35-37). However, neither of**
343 **the two clones harbored such mutation (not shown), although the presence of other drug-resistant**
344 **mutations at the level of the FGFR1 receptor cannot be ruled out. In addition, we excluded the**
345 **activation of efflux pumps as a mechanism of resistance leading to a reduced accumulation of**
346 **BGJ398 in H1581R clones; indeed, no difference in the intracellular concentration of the drug**
347 **emerged between the resistant clones and the parental cells (Figure 5C).**

348 **Interestingly, both the AKT and MAPK pathways remained activated in H1581R clones in the**
349 **presence of BGJ398 in contrast with the parental cells (Figure 5D); in addition, we found that *NRAS***
350 **was amplified in both clones, i.e. 61 copies for H1581R1 and 69 copies for H1581R2 cells vs 4.2**
351 **copies for H1581 cells (Figure 5E), likely contributing to the resistant phenotype.**

353 **UPR1376 inhibits cell growth in H1581R cell clones and this effect is enhanced by the** 354 **combination with the MEK1/2 inhibitor trametinib**

355 H1581R1 and H1581R2 cell clones were then analyzed for their sensitivity to UPR1371-UPR1376
356 in comparison with FIIN-2. As shown in Figure 6A5C, the irreversible reference compound slightly
357 affected cell proliferation; among our compounds, only UPR1376 showed a marked anti-tumor
358 activity, inhibiting cell proliferation almost completely at 1 μ M.

359 We therefore focused our attention on UPR1376. We treated the resistant cell clones with
360 increasing concentrations of UPR1376 and demonstrated that this compound inhibited cell
361 proliferation in a dose-dependent manner in both H1581R1 and H1581R2 cells, with IC₅₀ values of
362 220 and 312 nM, respectively (Figure 6B5D). In addition, we evaluated whether UPR1376 was
363 effective in inhibiting cell growth also in 3D systems. As shown in Figure 6C5E, H1581R1 cells
364 were capable of growing as tumor spheroids in the presence of BGJ398. FIIN-2 had no growth-
365 inhibitory effect; in contrast, UPR1376 induced a complete block of cell growth, confirming its
366 ability to circumvent resistance to BGJ398 in H1581-derived cells.

367 Then we evaluated the effects of UPR1376 on FGFR1 signaling in comparison with BGJ398 and
368 FIIN-2 (Figure 67A). As expected, BGJ398 did not inhibit FGFR1 nor affected downstream
369 pathways in resistant clones. FIIN-2 marginally affected FGFR1 phosphorylation and the
370 downstream signaling, while marginally affected FGFR1 phosphorylation, failed to down-regulate
371 the downstream signaling, thus justifying its low inhibitory activity on cell proliferation on H1581R
372 clones. In contrast, UPR1376 significantly inhibited FGFR1 phosphorylation/activation in both cell
373 clones and, to some extent, also affected downstream pathways. Importantly In particular, UPR1376
374 down-regulated the AKT pathway, as indicated by the significant reduction of both p-AKT and p-
375 p70S6K levels; however, no inhibition on ERK1/2 phosphorylation was observed, suggesting that
376 reactivation of the MAPK pathway occurred independently of FGFR1, likely due the emergence of
377 NRAS amplification (38).that additional alterations, independent of FGFR1, may have occurred,
378 which might sustain the activation of the MAPK pathway in BGJ398-resistant cell clones.

379 These findings suggest that H1581R1 and H1581R2 cell clones still rely on FGFR1 and
380 downstream AKT signaling for their proliferation. However, it is worth noting that the resistant
381 clones were less sensitive to UPR1376 than the parental cells (IC₅₀ values of 220 nM for H1581R1
382 clone and 312 nM for H1581R2 clone, respectively vs 0.8 nM for inhibitor-sensitive H1581 cells),
383 suggesting that a contribution to cell growth in the resistant cells may also derive from MAPK
384 signaling through FGFR1-independent mechanisms.

385 The persistent activation of the MAPK pathway in BGJ398-resistant cell clones provided the
386 rationale for combining UPR1376 with trametinib, a highly specific inhibitor of MEK1/2 proteins,
387 which are components of the MAPK signaling. H1581R1 cells were exposed to increasing
388 concentrations of UPR1376 combined with a fixed concentration of trametinib, chosen on the base
389 of a dose-response curve of proliferation previously determined (not shown). According to the Bliss
390 experimental model, such combination produced synergistic anti-proliferative effects (Figure 67B).

391 The stronger efficacy of the combination over compared to the single treatments was associated
392 with the simultaneous down-regulation of the AKT pathway, mediated by UPR1376 through
393 FGFR1 inhibition, and the MAPK pathway, mediated by trametinib (Figure 67C). Of note,
394 trametinib increased AKT phosphorylation, which was completely inhibited by UPR1376 treatment.
395 Altogether these results suggest that treatment with UPR1376 may be an effective therapeutic
396 approach to overcome resistance to BGJ398 and that its efficacy may be further improved by
397 combination with trametinib when the resistance is also associated with persistent activation of the
398 MAPK pathway.

400 Discussion

401 Aberrant activation of FGFR signaling has been demonstrated to play a key role in sustaining the
402 growth of multiple cancers, including SQCLC, thereby offering novel opportunities for targeted
403 therapeutic intervention. Both non-selective and selective FGFR inhibitors have shown strong anti-
404 tumor activity in pre-clinical studies and are currently being evaluated in clinical trials for the
405 treatment of patients with tumors carrying FGFR alterations. Although promising results are

406 emerging from these studies, several challenges are being faced, including the selection of
407 patients most likely to respond to FGFR inhibitors, the management of toxicity profiles, and the
408 appearance of drug resistance (17, 22).

409 Recently, the development of irreversible FGFR inhibitors has received growing attention due to
410 their increased efficiency, functional selectivity, and ability to circumvent acquired resistance
411 (39).

412 In this study, starting from 1-(4-aminobenzyl)-pyrimido[4,5-d] pyrimidin-2-one core of FIIN-2, we
413 synthesized a set of four inhibitors of FGFR in which the acrylamide warhead present in FIIN-2 was
414 replaced by a 3-APA group (i.e., UPR1371), potentially able to generate an acrylamide in cancer
415 cells (30), or by activated acetamides (i.e., UPR1372, 1373 and 1376), potentially able to alkylate
416 the P-loop cysteine of FGFR by nucleophilic substitution. In LENTI-4 cells, a FGFR1-over-
417 expressing SQCLC cell model generated in our lab, we found that incubation with UPR1371 failed
418 to give persistent inhibition of FGFR1 suggesting that, in this SQCLC cell model, the conversion of
419 the 3-APA group in acrylamide did not occur. Also the 2-(imidazol-2-ylthio)acetamide UPR1372
420 and the 2-(tetrazol-5-ylthio)acetamide UPR1373 failed to irreversibly inhibit FGFR1. In fact, 8
421 hours after their removal from the treated cells, the recovery of FGFR1 activity was nearly
422 complete, with phosphorylation levels approaching (UPR1372, UPR1373) or overcoming
423 (UPR1371) the 90 % of the control. The heteroarylthio acetamide group of UPR1372 and UPR1373
424 had been devised as warheads with very low reactivity; the present results show that higher
425 reactivity is needed to get irreversible inhibition of FGFR. On the other hand, the chloroacetamide
426 derivative UPR1376 was able to maintain FGFR1 significantly inhibited after its removal from the
427 cells. The comparison of the auto-phosphorylation levels of FGFR at 8 hours between UPR1376
428 (33% vs control) and FIIN-2 (49% vs control) indicated that the former compound was more
429 effective than the latter in irreversibly inhibiting FGFR1. In light of **this** **these** data, taking into
430 consideration the well-known reactivity of chloroacetamides toward thiols in solution (40), and
431 within the kinase active site (41), we speculated that the higher activity of UPR1376 may arise from
432 a more efficient alkylation of the P-loop cysteine of FGFR1 compared to the FIIN-2 compound.
433 Although additional experiments have to be performed to validate this hypothesis, a covalent
434 interaction **with** **between** FGFR1 and UPR1376 appears very likely. **The good metabolic stability**
435 **displayed by UPR1376 in cellular medium suggests that this compound might be able to engage**
436 **FGFR in the malignant tissue when administered *in vivo*. On support of this, an EGFR inhibitor**
437 **featured by a similar chloroacetamide warhead has been successfully used in the treatment of a**
438 **mouse xenograft model of NSCLC (42).**

439 In light of the prominent reactivity of chloroacetamide, we preliminary evaluated the toxicity of
440 UPR1376 by testing it on SQCLC SKMES-1 cells expressing low levels of FGFR1. This compound
441 did not affect **the** proliferation of SKMES-1 cells up to 1 μ M (Supplementary Figure 1), similarly to
442 what had been observed for BGJ-398 and FIIN-2, indicating the selective targeting of FGFR1 and
443 its isoforms.

444 UPR1376 demonstrated a significant anti-proliferative activity in H1581 NSCLC cells harboring
445 FGFR1 amplification **in** both **in** 2D and 3D systems. Most importantly, UPR1376 was shown to
446 restore sensitivity to FGFR1 inhibition in H1581-**derived** cell clones generated through chronic
447 exposure to BGJ398 and become resistant to both BGJ398 and the irreversible reference inhibitor
448 FIIN-2.

449 To date, multiple mechanisms of resistance to FGFR inhibitors have been described, mostly in pre-
450 clinical studies, which can be related to the activation of compensatory signaling or the appearance
451 of gatekeeper mutations in the FGFR receptors themselves (14).

452 In H1581 cells sensitive to FGFR1 inhibition UPR1376, as well as BGJ398 and FIIN-2, inhibited
453 either the MAPK or the AKT/MTOR pathways downstream of FGFR1. In H1581R cell clones,
454 resistance to BGJ398 was associated with the maintenance of FGFR1 phosphorylation and with the
455 persistent activation of both signaling cascades. **The inability of BGJ398 to suppress FGFR1**
456 **activation was not due to the acquisition of the gatekeeper V561M mutation, previously shown to**

457 confer resistance to FGFR inhibitors in different cancer models (35-37). However, we cannot
458 exclude the presence of other mutations at FGFR1 level. Recently, the increased expression of the
459 drug efflux transporter ABCG2 has been identified as an additional mechanism of resistance to the
460 selective FGFR inhibitor AZD4547 (43). However, it does not seem to be the case for H1581R cell
461 clones, since the intracellular accumulation of BGJ398 in these cells is comparable to that observed
462 in the parental cells. These clones also acquired cross-resistance to the irreversible inhibitor FIIN-2,
463 which failed to inhibit FGFR1 phosphorylation and left unaffected both the MAPK and the AKT
464 signaling. UPR1376 inhibited cell proliferation in both H1581R clones thanks to its ability to
465 significantly inhibit phosphorylation/activation of FGFR1 and the downstream AKT/mTOR
466 pathway. H1581R cell clones acquired cross-resistance also to the irreversible inhibitor FIIN-2.
467 UPR1376, in contrast with BGJ398 and FIIN-2, significantly inhibited the
468 phosphorylation/activation of FGFR1 and the downstream AKT/mTOR pathway, thus impairing
469 cell proliferation. A prominent role for AKT/mTOR in FGFR signaling has been previously
470 demonstrated in cancer in a number of studies (24, 44-46). In addition, activation of AKT in cancer
471 cell lines carrying activating FGFR alterations has been reported as a mechanism of acquired
472 resistance to BGJ398, which can be efficaciously reverted by treatment with an AKT inhibitor (47).
473 In H1581R clones, not AKT but MAPK signaling was activated independently of FGFR1, being
474 ERK1/2 phosphorylation maintained also in the presence of UPR1376-mediated inhibition of
475 FGFR1. Interestingly we found that such up-regulation was associated with *NRAS* amplification.
476 The persistent activation of MAPK signaling likely contributes to BGJ398 resistance in H1581R
477 clones, also to some extent reducing to some extent their sensitivity to UPR1376 in comparison
478 with the parental cells. Indeed, the anti-tumor efficacy of UPR1376 was greatly improved by the
479 combination with the specific MEK1/2 inhibitor trametinib. Recently, reactivation of MAPK
480 pathway, mediated by *NRAS* amplification or *MET* transcriptional regulation, has been linked to the
481 emergence of resistance to FGFR inhibitors in FGFR1-amplified lung cancer cell models (38). In
482 these cells, co-treatment with trametinib or the MET inhibitor crizotinib restored the sensitivity to
483 BGJ398 by inhibiting the MAPK signaling in a direct or indirect fashion, respectively.
484 It is worth noting that treatment with trametinib alone, while inhibiting the MAPK signaling,
485 increased AKT phosphorylation/activation in H1581R cells, resulting in a limited efficacy;
486 UPR1376, blocking FGFR1 signaling, completely reverted reversed this effect leading to a
487 synergistic impairment of cell growth. Based on these findings, it is conceivable that the
488 simultaneous inhibition of FGFR/AKT and MAPK signaling is required to achieve a significant
489 anti-proliferative response, overcoming the resistance to FGFR inhibitors.
490 Collectively our results suggest the concomitance of different mechanisms of resistance in H1581R
491 cell clones. This is line with the results from a recent study describing a SQCLC cell model of
492 acquired resistance to FGFR inhibitors, in which the activation of the MET/MAPK axis co-exists
493 with an independent change of the *AKT1* gene leading to the activation of AKT signaling (48).
494 These observations support the notion that the emergence of multiple genetic lesions within the
495 same cells may represent a common mechanism of resistance requiring a combined therapy
496 intervention to restore tumor cell responsiveness.

498 Conclusions

499 Because of the recognized role of FGFR signaling in cancer progression, intensive efforts are being
500 made to develop effective FGFR-targeted therapies, which are especially urgent for challenging-to-
501 treat cancers, like SQCLC, that still have few treatment options available. In this study, among the
502 reported compounds, chloroacetamide UPR1376 emerged as a promising irreversible inhibitor of
503 FGFR able to block proliferation of FGFR1-amplified H1581 cells with a potency higher than
504 BGJ398, while sparing FGFR1 low-expressing cells. Interestingly, in two distinct H1581-derived
505 clones resistant to BGJ398, UPR1376 inhibited proliferation at nanomolar concentration, an effect
506 that was strongly enhanced by trametinib. Collectively, our results suggest that the insertion of a
507 chloroacetamide warhead on a suitable scaffold is a viable strategy to find a novel generation of

508 FGFR inhibitors, which may offer new therapeutic opportunities for treating SQCLC patients with
509 FGFR alterations and overcoming acquired resistance.

510

511 **Acknowledgments**

512 This work was supported by Associazione Italiana per la Ricerca sul Cancro (AIRC), Milan grant
513 IG 14214 (to A. Ardizzoni), Associazione Volontaria Promozione Ricerca Tumori
514 (A.VO.PRO.RI.T.) (Parma), Associazione Augusto per la Vita (Novellara, Reggio Emilia),
515 Associazione di Mano in Mano (Parma), and Associazione Marta Nurizzo, Brugherio (MI). The
516 funders had no role in study design, data collection and analysis, decision to publish, or preparation
517 of the manuscript.

518

519 **Author Contributions Statement**

520 Conception and design: MM, PGP, AA; cell biology and molecular biology experiments: CF, MB,
521 SLM, DC, RM, MG; chemical synthesis: NB, RC, GM; chemical analysis: FF; writing of the
522 manuscript: CF, AL; review of the manuscript: MB, AR; study supervision: MM, PGP, MT. All the
523 authors contributed to revise the manuscript and approved the final version for publication.

524

525 **Conflict of Interest Statement**

526 The authors declare no conflicts of interest.

527

528 **References**

- 529 1. Turner N, Grose R. Fibroblast growth factor signalling: from development to cancer.
530 *Nat Rev Cancer* (2010) 10(2):116-29. Epub 2010/01/23. doi: 10.1038/nrc2780
531 nrc2780 [pii]. PubMed PMID: 20094046.
- 532 2. Touat M, Ileana E, Postel-Vinay S, Andre F, Soria JC. Targeting FGFR Signaling in
533 Cancer. *Clin Cancer Res* (2015) 21(12):2684-94. Epub 2015/06/17. doi: 10.1158/1078-
534 0432.CCR-14-2329
535 21/12/2684 [pii]. PubMed PMID: 26078430.
- 536 3. Helsten T, Elkin S, Arthur E, Tomson BN, Carter J, Kurzrock R. The FGFR
537 Landscape in Cancer: Analysis of 4,853 Tumors by Next-Generation Sequencing. *Clin Cancer*
538 *Res* (2016) 22(1):259-67. Epub 2015/09/17. doi: 10.1158/1078-0432.CCR-14-3212
539 1078-0432.CCR-14-3212 [pii]. PubMed PMID: 26373574.
- 540 4. Weiss J, Sos ML, Seidel D, Peifer M, Zander T, Heuckmann JM, et al. Frequent and
541 focal FGFR1 amplification associates with therapeutically tractable FGFR1 dependency in
542 squamous cell lung cancer. *Sci Transl Med* (2010) 2(62):62ra93. Epub 2010/12/17. doi:
543 10.1126/scitranslmed.3001451
544 2/62/62ra93 [pii]. PubMed PMID: 21160078; PubMed Central PMCID: PMC3990281.
- 545 5. Dutt A, Ramos AH, Hammerman PS, Mermel C, Cho J, Sharifnia T, et al. Inhibitor-
546 sensitive FGFR1 amplification in human non-small cell lung cancer. *PLoS One* (2011)
547 6(6):e20351. Epub 2011/06/15. doi: 10.1371/journal.pone.0020351
548 PONE-D-11-00027 [pii]. PubMed PMID: 21666749; PubMed Central PMCID: PMC3110189.
- 549 6. Brahmer J, Reckamp KL, Baas P, Crino L, Eberhardt WE, Poddubskaya E, et al.
550 Nivolumab versus Docetaxel in Advanced Squamous-Cell Non-Small-Cell Lung Cancer. *N*
551 *Engl J Med* (2015) 373(2):123-35. Epub 2015/06/02. doi: 10.1056/NEJMoa1504627. PubMed
552 PMID: 26028407; PubMed Central PMCID: PMC4681400.
- 553 7. Garon EB, Rizvi NA, Hui R, Leighl N, Balmanoukian AS, Eder JP, et al.
554 Pembrolizumab for the treatment of non-small-cell lung cancer. *N Engl J Med* (2015)
555 372(21):2018-28. Epub 2015/04/22. doi: 10.1056/NEJMoa1501824. PubMed PMID: 25891174.
- 556 8. Herbst RS, Baas P, Kim DW, Felip E, Perez-Gracia JL, Han JY, et al. Pembrolizumab
557 versus docetaxel for previously treated, PD-L1-positive, advanced non-small-cell lung cancer

- 558 (KEYNOTE-010): a randomised controlled trial. *Lancet* (2016) 387(10027):1540-50. Epub
559 2015/12/30. doi: 10.1016/S0140-6736(15)01281-7
560 S0140-6736(15)01281-7 [pii]. PubMed PMID: 26712084.
- 561 9. Rittmeyer A, Barlesi F, Waterkamp D, Park K, Ciardiello F, von Pawel J, et al.
562 Atezolizumab versus docetaxel in patients with previously treated non-small-cell lung cancer
563 (OAK): a phase 3, open-label, multicentre randomised controlled trial. *Lancet* (2017)
564 389(10066):255-65. Epub 2016/12/17. doi: S0140-6736(16)32517-X [pii]
565 10.1016/S0140-6736(16)32517-X. PubMed PMID: 27979383.
- 566 10. Dieci MV, Arnedos M, Andre F, Soria JC. Fibroblast growth factor receptor inhibitors
567 as a cancer treatment: from a biologic rationale to medical perspectives. *Cancer Discov* (2013)
568 3(3):264-79. Epub 2013/02/19. doi: 10.1158/2159-8290.CD-12-0362
569 2159-8290.CD-12-0362 [pii]. PubMed PMID: 23418312.
- 570 11. Gavine PR, Mooney L, Kilgour E, Thomas AP, Al-Kadhimi K, Beck S, et al. AZD4547:
571 an orally bioavailable, potent, and selective inhibitor of the fibroblast growth factor receptor
572 tyrosine kinase family. *Cancer Res* (2012) 72(8):2045-56. Epub 2012/03/01. doi: 10.1158/0008-
573 5472.CAN-11-3034
574 0008-5472.CAN-11-3034 [pii]. PubMed PMID: 22369928.
- 575 12. Perera TPS, Jovcheva E, Mevellec L, Vialard J, De Lange D, Verhulst T, et al.
576 Discovery and Pharmacological Characterization of JNJ-42756493 (Erdafitinib), a
577 Functionally Selective Small-Molecule FGFR Family Inhibitor. *Mol Cancer Ther* (2017)
578 16(6):1010-20. Epub 2017/03/28. doi: 10.1158/1535-7163.MCT-16-0589
579 1535-7163.MCT-16-0589 [pii]. PubMed PMID: 28341788.
- 580 13. Nogova L, Sequist LV, Perez Garcia JM, Andre F, Delord JP, Hidalgo M, et al.
581 Evaluation of BGJ398, a Fibroblast Growth Factor Receptor 1-3 Kinase Inhibitor, in Patients
582 With Advanced Solid Tumors Harboring Genetic Alterations in Fibroblast Growth Factor
583 Receptors: Results of a Global Phase I, Dose-Escalation and Dose-Expansion Study. *J Clin*
584 *Oncol* (2017) 35(2):157-65. Epub 2016/11/22. doi: 10.1200/JCO.2016.67.2048 [pii]
585 10.1200/JCO.2016.67.2048. PubMed PMID: 27870574.
- 586 14. Chae YK, Ranganath K, Hammerman PS, Vaklavas C, Mohindra N, Kalyan A, et al.
587 Inhibition of the fibroblast growth factor receptor (FGFR) pathway: the current landscape
588 and barriers to clinical application. *Oncotarget* (2017) 8(9):16052-74. Epub 2016/12/29. doi:
589 10.18632/oncotarget.14109
590 14109 [pii]. PubMed PMID: 28030802; PubMed Central PMCID: PMC5362545.
- 591 15. Paik PK, Rudin CM. Missing the mark in FGFR1-amplified squamous cell cancer of
592 the lung. *Cancer* (2016) 122(19):2938-40. Epub 2016/06/18. doi: 10.1002/cncr.30131. PubMed
593 PMID: 27315203.
- 594 16. Paik PK, Shen R, Berger MF, Ferry D, Soria JC, Mathewson A, et al. A Phase Ib
595 Open-Label Multicenter Study of AZD4547 in Patients with Advanced Squamous Cell Lung
596 Cancers. *Clin Cancer Res* (2017) 23(18):5366-73. Epub 2017/06/16. doi: 10.1158/1078-
597 0432.CCR-17-0645
598 1078-0432.CCR-17-0645 [pii]. PubMed PMID: 28615371; PubMed Central PMCID:
599 PMC5600836.
- 600 17. Goyal L, Saha SK, Liu LY, Siravegna G, Leshchiner I, Ahronian LG, et al. Polyclonal
601 Secondary FGFR2 Mutations Drive Acquired Resistance to FGFR Inhibition in Patients with
602 FGFR2 Fusion-Positive Cholangiocarcinoma. *Cancer Discov* (2017) 7(3):252-63. Epub
603 2016/12/31. doi: 10.1158/2159-8290.CD-16-1000
604 2159-8290.CD-16-1000 [pii]. PubMed PMID: 28034880; PubMed Central PMCID:
605 PMC5433349.
- 606 18. Tan L, Wang J, Tanizaki J, Huang Z, Aref AR, Rusan M, et al. Development of
607 covalent inhibitors that can overcome resistance to first-generation FGFR kinase inhibitors.

- 608 *Proc Natl Acad Sci U S A* (2014) 111(45):E4869-77. Epub 2014/10/29. doi:
609 10.1073/pnas.1403438111
610 1403438111 [pii]. PubMed PMID: 25349422; PubMed Central PMCID: PMC4234547.
- 611 19. Carmi C, Mor M, Petronini PG, Alfieri RR. Clinical perspectives for irreversible
612 tyrosine kinase inhibitors in cancer. *Biochem Pharmacol* (2012) 84(11):1388-99. Epub
613 2012/08/14. doi: 10.1016/j.bcp.2012.07.031
614 S0006-2952(12)00513-8 [pii]. PubMed PMID: 22885287.
- 615 20. Lonsdale R, Ward RA. Structure-based design of targeted covalent inhibitors. *Chem*
616 *Soc Rev* (2018) 47(11):3816-30. Epub 2018/04/06. doi: 10.1039/c7cs00220c. PubMed PMID:
617 29620097.
- 618 21. Singh J, Petter RC, Baillie TA, Whitty A. The resurgence of covalent drugs. *Nat Rev*
619 *Drug Discov* (2011) 10(4):307-17. Epub 2011/04/02. doi: 10.1038/nrd3410
620 nrd3410 [pii]. PubMed PMID: 21455239.
- 621 22. Venetsanakos E, Brameld KA, Phan VT, Verner E, Owens TD, Xing Y, et al. The
622 Irreversible Covalent Fibroblast Growth Factor Receptor Inhibitor PRN1371 Exhibits
623 Sustained Inhibition of FGFR after Drug Clearance. *Mol Cancer Ther* (2017) 16(12):2668-76.
624 Epub 2017/10/06. doi: 10.1158/1535-7163.MCT-17-0309
625 1535-7163.MCT-17-0309 [pii]. PubMed PMID: 28978721.
- 626 23. Brameld KA, Owens TD, Verner E, Venetsanakos E, Bradshaw JM, Phan VT, et al.
627 Discovery of the Irreversible Covalent FGFR Inhibitor 8-(3-(4-Acryloylpiperazin-1-
628 yl)propyl)-6-(2,6-dichloro-3,5-dimethoxyphenyl)-2-(methylamino)pyrido[2,3-d]pyrimidin-
629 7(8H)-one (PRN1371) for the Treatment of Solid Tumors. *J Med Chem* (2017) 60(15):6516-27.
630 Epub 2017/07/01. doi: 10.1021/acs.jmedchem.7b00360. PubMed PMID: 28665128.
- 631 24. Fumarola C, Cretella D, La Monica S, Bonelli MA, Alfieri R, Caffarra C, et al.
632 Enhancement of the anti-tumor activity of FGFR1 inhibition in squamous cell lung cancer by
633 targeting downstream signaling involved in glucose metabolism. *Oncotarget* (2017)
634 8(54):91841-59. Epub 2017/12/02. doi: 10.18632/oncotarget.19279
635 19279 [pii]. PubMed PMID: 29190880; PubMed Central PMCID: PMC5696146.
- 636 25. Fumarola C, Caffarra C, La Monica S, Galetti M, Alfieri RR, Cavazzoni A, et al.
637 Effects of sorafenib on energy metabolism in breast cancer cells: role of AMPK-mTORC1
638 signaling. *Breast Cancer Res Treat* (2013) 141(1):67-78. Epub 2013/08/22. doi: 10.1007/s10549-
639 013-2668-x. PubMed PMID: 23963659.
- 640 26. Cavazzoni A, Petronini PG, Galetti M, Roz L, Andriani F, Carbognani P, et al. Dose-
641 dependent effect of FHIT-inducible expression in Calu-1 lung cancer cell line. *Oncogene*
642 (2004) 23(52):8439-46. Epub 2004/09/14. doi: 10.1038/sj.onc.1207847
643 1207847 [pii]. PubMed PMID: 15361849.
- 644 27. Goldoni M, Johansson C. A mathematical approach to study combined effects of
645 toxicants in vitro: evaluation of the Bliss independence criterion and the Loewe additivity
646 model. *Toxicol In Vitro* (2007) 21(5):759-69. Epub 2007/04/11. doi: S0887-2333(07)00067-7
647 [pii]
648 10.1016/j.tiv.2007.03.003. PubMed PMID: 17420112.
- 649 28. Bonelli MA, Cavazzoni A, Saccani F, Alfieri RR, Quaini F, La Monica S, et al.
650 Inhibition of PI3K Pathway Reduces Invasiveness and Epithelial-to-Mesenchymal Transition
651 in Squamous Lung Cancer Cell Lines Harboring PIK3CA Gene Alterations. *Mol Cancer Ther*
652 (2015) 14(8):1916-27. Epub 2015/05/28. doi: 10.1158/1535-7163.MCT-14-0892
653 1535-7163.MCT-14-0892 [pii]. PubMed PMID: 26013318.
- 654 29. Chen W, Wong C, Vosburgh E, Levine AJ, Foran DJ, Xu EY. High-throughput image
655 analysis of tumor spheroids: a user-friendly software application to measure the size of
656 spheroids automatically and accurately. *J Vis Exp* (2014) (89). Epub 2014/07/22. doi:
657 10.3791/51639. PubMed PMID: 25046278; PubMed Central PMCID: PMC4212916.

- 658 30. Carmi C, Galvani E, Vacondio F, Rivara S, Lodola A, Russo S, et al. Irreversible
659 inhibition of epidermal growth factor receptor activity by 3-aminopropanamides. *J Med*
660 *Chem* (2012) 55(5):2251-64. Epub 2012/01/28. doi: 10.1021/jm201507x. PubMed PMID:
661 22280453.
- 662 31. Carmi C, Cavazzoni A, Vezzosi S, Bordi F, Vacondio F, Silva C, et al. Novel
663 irreversible epidermal growth factor receptor inhibitors by chemical modulation of the
664 cysteine-trap portion. *J Med Chem* (2010) 53(5):2038-50. Epub 2010/02/16. doi:
665 10.1021/jm901558p. PubMed PMID: 20151670.
- 666 32. Vacondio F, Carmi C, Galvani E, Bassi M, Silva C, Lodola A, et al. Long-lasting
667 inhibition of EGFR autophosphorylation in A549 tumor cells by intracellular accumulation of
668 non-covalent inhibitors. *Bioorg Med Chem Lett* (2013) 23(19):5290-4. Epub 2013/08/31. doi:
669 10.1016/j.bmcl.2013.08.008
670 S0960-894X(13)00937-2 [pii]. PubMed PMID: 23988354.
- 671 33. Castelli R, Bozza N, Cavazzoni A, Bonelli M, Vacondio F, Ferlenghi F, et al. Balancing
672 reactivity and antitumor activity: heteroarylthioacetamide derivatives as potent and time-
673 dependent inhibitors of EGFR. *Eur J Med Chem* (2019) 162:507-24. Epub 2018/11/26. doi:
674 S0223-5234(18)30988-7 [pii]
675 10.1016/j.ejmech.2018.11.029. PubMed PMID: 30472599.
- 676 34. Galetti M, Alfieri RR, Cavazzoni A, La Monica S, Bonelli M, Fumarola C, et al.
677 Functional characterization of gefitinib uptake in non-small cell lung cancer cell lines.
678 *Biochem Pharmacol* (2010) 80(2):179-87. Epub 2010/04/07. doi: 10.1016/j.bcp.2010.03.033
679 S0006-2952(10)00221-2 [pii]. PubMed PMID: 20363215.
- 680 35. Sohl CD, Ryan MR, Luo B, Frey KM, Anderson KS. Illuminating the molecular
681 mechanisms of tyrosine kinase inhibitor resistance for the FGFR1 gatekeeper mutation: the
682 Achilles' heel of targeted therapy. *ACS Chem Biol* (2015) 10(5):1319-29. Epub 2015/02/17. doi:
683 10.1021/acscmbio.5b00014. PubMed PMID: 25686244; PubMed Central PMCID:
684 PMC4533833.
- 685 36. Ryan MR, Sohl CD, Luo B, Anderson KS. The FGFR1 V561M Gatekeeper Mutation
686 Drives AZD4547 Resistance Through STAT3 Activation and EMT. *Mol Cancer Res* (2018).
687 Epub 2018/09/28. doi: 10.1158/1541-7786.MCR-18-0429
688 1541-7786.MCR-18-0429 [pii]. PubMed PMID: 30257990.
- 689 37. Cowell JK, Qin H, Hu T, Wu Q, Bhole A, Ren M. Mutation in the FGFR1 tyrosine
690 kinase domain or inactivation of PTEN is associated with acquired resistance to FGFR
691 inhibitors in FGFR1-driven leukemia/lymphomas. *Int J Cancer* (2017) 141(9):1822-9. Epub
692 2017/06/25. doi: 10.1002/ijc.30848. PubMed PMID: 28646488; PubMed Central PMCID:
693 PMC5850950.
- 694 38. Malchers F, Ercanoglu M, Schutte D, Castiglione R, Tischler V, Michels S, et al.
695 Mechanisms of Primary Drug Resistance in FGFR1-Amplified Lung Cancer. *Clin Cancer Res*
696 (2017) 23(18):5527-36. Epub 2017/06/21. doi: 10.1158/1078-0432.CCR-17-0478
697 1078-0432.CCR-17-0478 [pii]. PubMed PMID: 28630215.
- 698 39. Barf T, Kaptein A. Irreversible protein kinase inhibitors: balancing the benefits and
699 risks. *J Med Chem* (2012) 55(14):6243-62. Epub 2012/05/25. doi: 10.1021/jm3003203. PubMed
700 PMID: 22621397.
- 701 40. Flanagan ME, Abramite JA, Anderson DP, Aulabaugh A, Dahal UP, Gilbert AM, et al.
702 Chemical and computational methods for the characterization of covalent reactive groups for
703 the prospective design of irreversible inhibitors. *J Med Chem* (2014) 57(23):10072-9. Epub
704 2014/11/07. doi: 10.1021/jm501412a. PubMed PMID: 25375838.
- 705 41. Kung A, Chen YC, Schimpl M, Ni F, Zhu J, Turner M, et al. Development of Specific,
706 Irreversible Inhibitors for a Receptor Tyrosine Kinase EphB3. *J Am Chem Soc* (2016)
707 138(33):10554-60. Epub 2016/08/02. doi: 10.1021/jacs.6b05483. PubMed PMID: 27478969.

- 708 42. Shindo N, Fuchida H, Sato M, Watari K, Shibata T, Kuwata K, et al. Selective and
 709 reversible modification of kinase cysteines with chlorofluoroacetamides. *Nat Chem Biol*
 710 (2019). Epub 2019/01/16. doi: 10.1038/s41589-018-0204-3
 711 10.1038/s41589-018-0204-3 [pii]. PubMed PMID: 30643284.
- 712 43. Kas SM, de Ruiter JR, Schipper K, Schut E, Bombardelli L, Wientjens E, et al.
 713 Transcriptomics and Transposon Mutagenesis Identify Multiple Mechanisms of Resistance to
 714 the FGFR Inhibitor AZD4547. *Cancer Res* (2018) 78(19):5668-79. Epub 2018/08/18. doi:
 715 10.1158/0008-5472.CAN-18-0757
 716 0008-5472.CAN-18-0757 [pii]. PubMed PMID: 30115694.
- 717 44. Starska K, Forma E, Lewy-Trenda I, Stasikowska-Kanicka O, Skora M, Brys M.
 718 Fibroblast growth factor receptor 1 and 3 expression is associated with regulatory PI3K/AKT
 719 kinase activity, as well as invasion and prognosis, in human laryngeal cancer. *Cell Oncol*
 720 (*Dordr*) (2018) 41(3):253-68. Epub 2018/01/05. doi: 10.1007/s13402-017-0367-z
 721 10.1007/s13402-017-0367-z [pii]. PubMed PMID: 29299828.
- 722 45. Hu Y, Lu H, Zhang J, Chen J, Chai Z. Essential role of AKT in tumor cells addicted to
 723 FGFR. *Anticancer Drugs* (2014) 25(2):183-8. Epub 2013/10/09. doi:
 724 10.1097/CAD.000000000000034. PubMed PMID: 24100276.
- 725 46. Dey JH, Bianchi F, Voshol J, Bonenfant D, Oakeley EJ, Hynes NE. Targeting
 726 fibroblast growth factor receptors blocks PI3K/AKT signaling, induces apoptosis, and
 727 impairs mammary tumor outgrowth and metastasis. *Cancer Res* (2010) 70(10):4151-62. Epub
 728 2010/05/13. doi: 10.1158/0008-5472.CAN-09-4479
 729 0008-5472.CAN-09-4479 [pii]. PubMed PMID: 20460524.
- 730 47. Datta J, Damodaran S, Parks H, Ocrainiciuc C, Miya J, Yu L, et al. Akt Activation
 731 Mediates Acquired Resistance to Fibroblast Growth Factor Receptor Inhibitor BGJ398. *Mol*
 732 *Cancer Ther* (2017) 16(4):614-24. Epub 2017/03/04. doi: 10.1158/1535-7163.MCT-15-1010
 733 1535-7163.MCT-15-1010 [pii]. PubMed PMID: 28255027; PubMed Central PMCID:
 734 PMC5539948.
- 735 48. Gimenez-Xavier P, Pros E, Aza A, Moran S, Tonda R, Esteve-Codina A, et al. Deep
 736 analysis of acquired resistance to FGFR1 inhibitor identifies MET and AKT activation and an
 737 expansion of AKT1 mutant cells. *Oncotarget* (2018) 9(59):31549-58. Epub 2018/08/25. doi:
 738 10.18632/oncotarget.25862
 739 25862 [pii]. PubMed PMID: 30140389; PubMed Central PMCID: PMC6101141.

741 Legends

742
 743 **Figure 1.** Chemical structures of relevant inhibitors of FGFR.

744
 745 **Figure 2.** (A) Chemical formulas of tested compounds. (B) Hypothesized conversion of 3-APA
 746 group of UPR1371 in acrylamide of FIIN-2. (C) Putative mechanism of action for acetamide
 747 derivatives UPR1372, UPR1373 and UPR1376. The leaving group installed on the acetamide
 748 fragment is colored in red.

749
 750 **Figure 3. Inhibitory effects of UPR1371-UPR1376 on FGFR1 auto-phosphorylation in**
 751 **LENTI-4 cells.** LENTI-4 cells, serum-deprived for 24 h, were pre-treated with 1 μ M BGJ398, FIIN-
 752 2 or the newly synthesized FGFR inhibitors (UPR1371-UPR1376). After 1 h, the cells were
 753 stimulated with FGF2 for further 15 min, or extensively washed with PBS and stimulated with
 754 FGF2 for 15 min after 8 h of incubation in fresh drug-free medium. At the end of the treatments, the
 755 cells were lysed and the protein extracts were analyzed by Western blotting for FGFR1 auto-
 756 phosphorylation. Results are representative of three independent experiments. The immunoreactive
 757 spots were quantified by densitometric analysis, ratios of p-FGFR/total FGFR were calculated and
 758 values, expressed as percent vs control, are reported.

759
760
761
762
763
764
765
766
767
768
769
770
771
772
773

Figure 4. Effects of BGJ398, FIIN-2, and UPR1371-UPR1376 on cell growth and FGFR1 signaling in H1581 cells. (A) H1581 cells were treated with increasing concentrations of the FGFR inhibitors (0.001nM-10µM) and after 72 h cell proliferation was assessed by MTT assay. The IC₅₀ values shown are means ±SD of at least three independent experiments. (B) H1581 cells were treated with the FGFR inhibitors at 1 µM for 6 h, and then protein lysates were analyzed by Western blotting for the indicated proteins. Results are representative of two independent experiments. (C) H1581 cells were grown as tumor spheroids in the absence or presence of BGJ398, FIIN-2 or UPR1376 at 10 nM. Spheroid volumes were measured at three days after seeding (T0), and after 4, 7, or 10 days of culture. The data are means ±SD of four independent determinations. **p<0.01, ***p<0.001, ****p<0.0001 for BGJ398 vs control; ###p<0.001, ####p<0.0001 for FIIN-2 vs control; §§§p<0.001, §§§§p<0.0001 for UPR1376 vs control. Representative images of tumor spheroids at 10 days are shown.

Figure 5. Characterization of BGJ398-resistant cell clones generated from H1581 cells. (A) H1581, H1581R1, and H1581R2 cells were incubated with increasing concentrations of BGJ398 (0.001 nM-10 µM). After 72 h, cell proliferation was assessed by MTT assay. The data are expressed as percent inhibition of cell proliferation vs control. (B) H1581, H1581R1, and H1581R2 cells were incubated in the absence or presence of 1 µM BGJ398, and after 6 h protein lysates were analyzed by Western blotting for FGFR1 phosphorylation. (C) H1581, H1581R1, and H1581R2 cells were incubated with 1 µM BGJ398. Intracellular compound content was measured after 6 h by LC/MS. Concentrations are expressed as pmol of compound per mg of protein, determined using Bradford assay. (D) H1581 cells and H1581R clones were treated as in B and protein lysates were analyzed by Western blotting for the indicated proteins. (E) Genomic DNA was extracted from H1581 cells and H1581R clones and analyzed for the presence of *NRAS* amplification by ddPCR. Results in A and C are means ± SD of three independent experiments. Results in B and D are representative of three independent experiments.

Figure 65. Effects of UPR1371-UPR1376 on cell growth in BGJ398-resistant H1581R1 and H1581R2 cell clones. (A) H1581, H1581R1, and H1581R2 cells were incubated with increasing concentrations of BGJ398 (0.001 nM-10 µM). After 72 h, cell proliferation was assessed by MTT assay. (B) H1581 cells and the resistant clones were incubated in the absence or presence of 1 µM BGJ398, and after 6 h protein lysates were analyzed by Western blotting for FGFR1 phosphorylation. (AC) H1581R1 and H1581R2 cells were incubated with FIIN-2 reference inhibitor or UPR1371-UPR1376 compounds at 1 µM. After 72 h, cell proliferation was assessed by MTT assay. (BD) H1581R1 and H1581R2 cells were incubated with increasing concentrations of UPR1376 (1-1000 nM). After 72 h, cell proliferation was assessed by MTT assay. (CE) H1581R1 cells were grown as tumor spheroids in the presence of 1 µM BGJ398, FIIN-2 or UPR1376. Spheroid volumes were measured at three days after seeding (T0), and after 4, 7, or 10 days of culture. **p<0.01, ****p<0.0001 vs BGJ398-treated cells. Representative images of tumor spheroids at 10 days are shown. The data in A, C, and BD are expressed as percent inhibition of cell proliferation vs control and are means ± SD of at least three independent experiments. Results in B are representative of three independent experiments. The data in CE are means ±SD of four independent determinations.

Figure 76. Effects of FGFR inhibitors on cell signaling and effects of UPR1376 combined with trametinib in BGJ398-resistant cell clones. (A) H1581R1 and H1581R2 cells were incubated in the absence or presence of 1 µM BGJ398, FIIN-2 or UPR1376. After 6 h the cells were lysed and the protein extracts were analyzed by Western blotting for the indicated proteins. (B) H1581R1 cells were incubated with increasing concentrations of UPR1376 (0.01-1000 nM) in combination

810 with 100 nM trametinib. After 72 h cell proliferation was assessed by MTT assay. The effect of the
 811 drug combination was evaluated using the Bliss interaction model. (C) H1581R1 cells were
 812 incubated with 1 μ M UPR1376, 100 nM trametinib or a combination of both. After 6 h the cells
 813 were lysed and the protein extracts were analyzed by Western blotting for the indicated proteins.
 814 Results are representative of three independent experiments.

815
816
817
818

819 **Table 1. Intracellular levels of selected FGFR inhibitors measured in LENTI-4 cells by**
 820 **LC/MS.** LENTI-4 cells were incubated with 1 μ M solution of titled compound for 1 h. Intracellular
 821 content was measured immediately after incubation and 8 h after removal of the compound from the
 822 medium by extensive washing by LC/MS. Concentrations are expressed as pmol of compound per
 823 mg of protein, determined using Bradford assay. Results are representative of two independent
 824 experiments.

825

Cpds	Intracellular concentration (pmol/mg prot)	
	1h	8h
BGJ398	1843	52
FIIN-2	1132	95
UPR1376	109	4

826
827
828

Figure 01.TIF

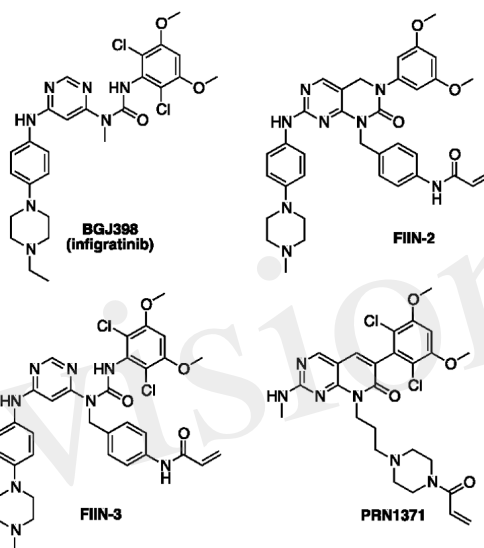


Figure 02.TIF

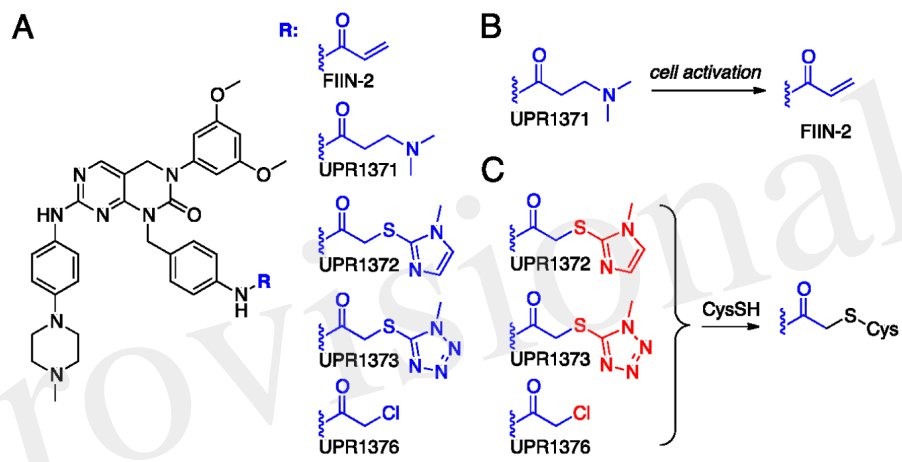


Figure 03.TIF

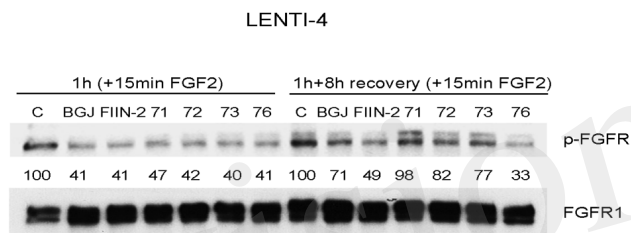


Figure 04.TIF

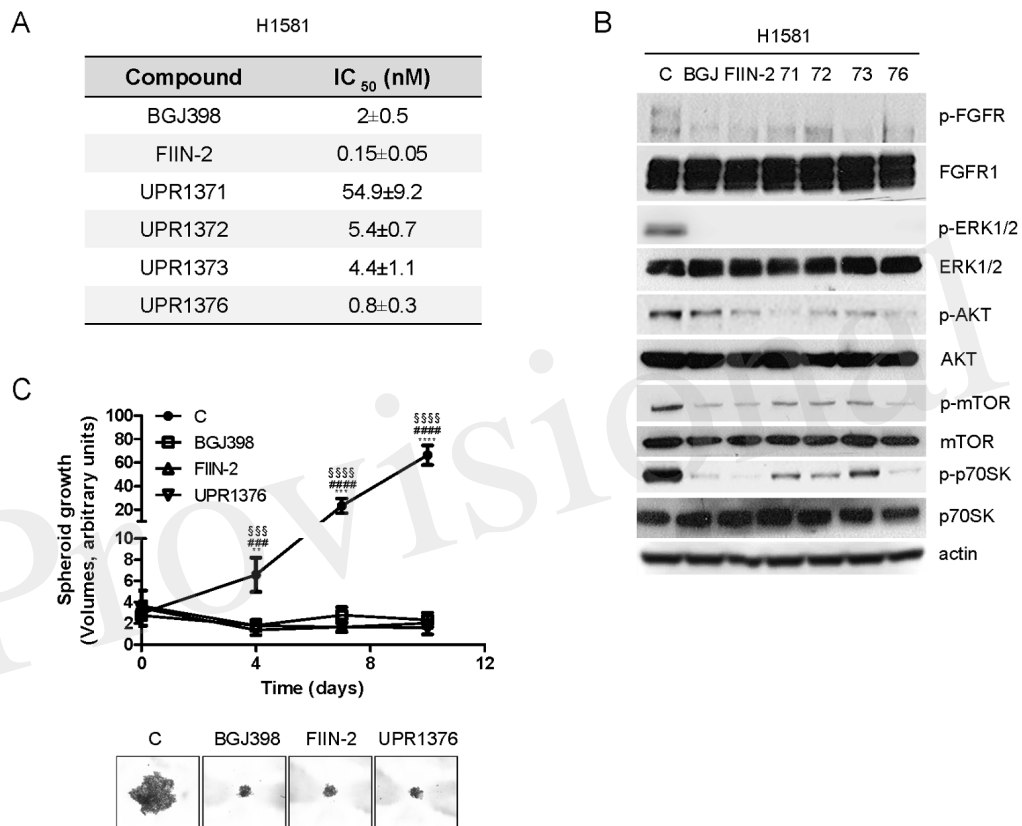


Figure 05.TIFF

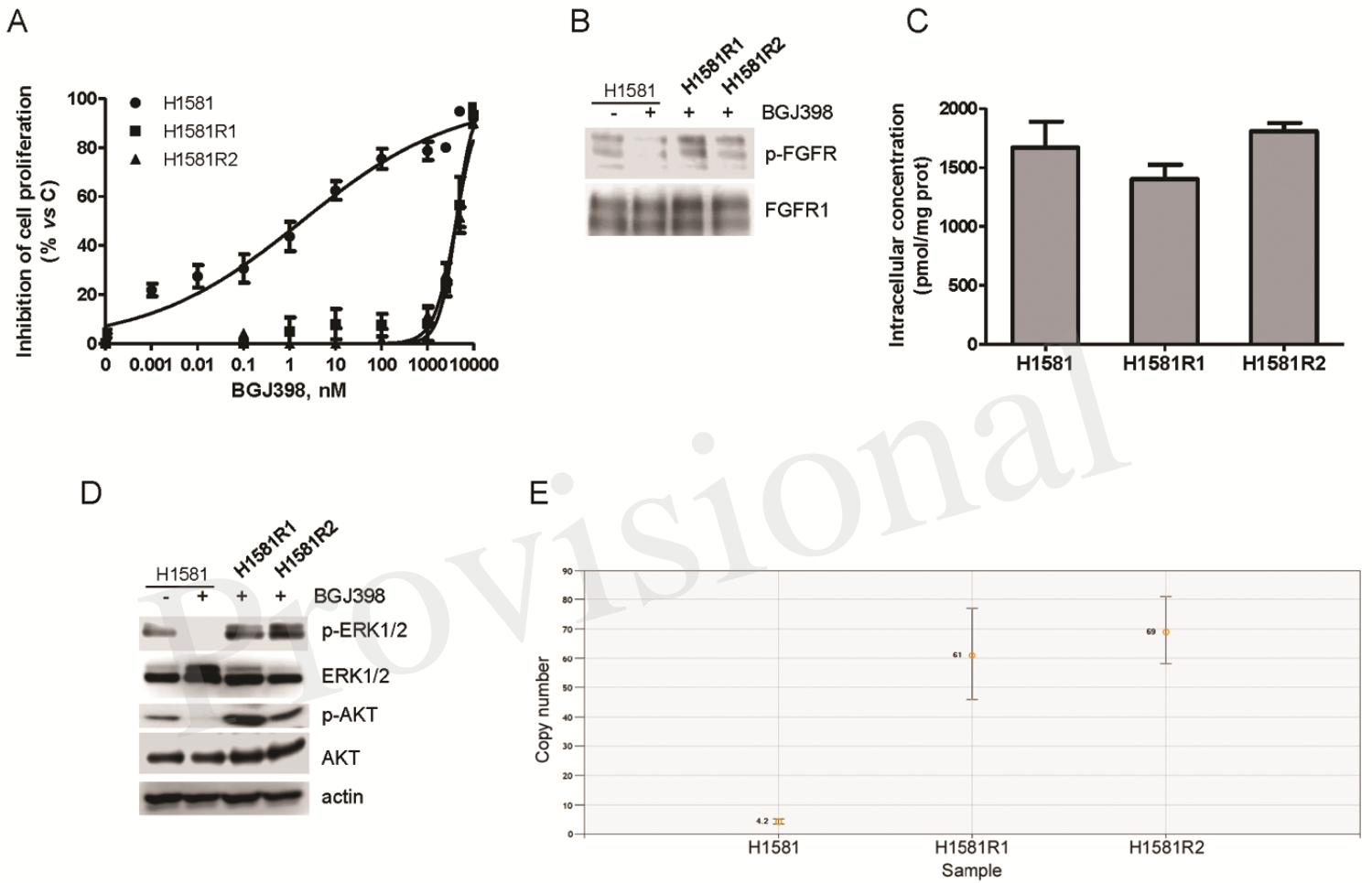


Figure 06.TIFF

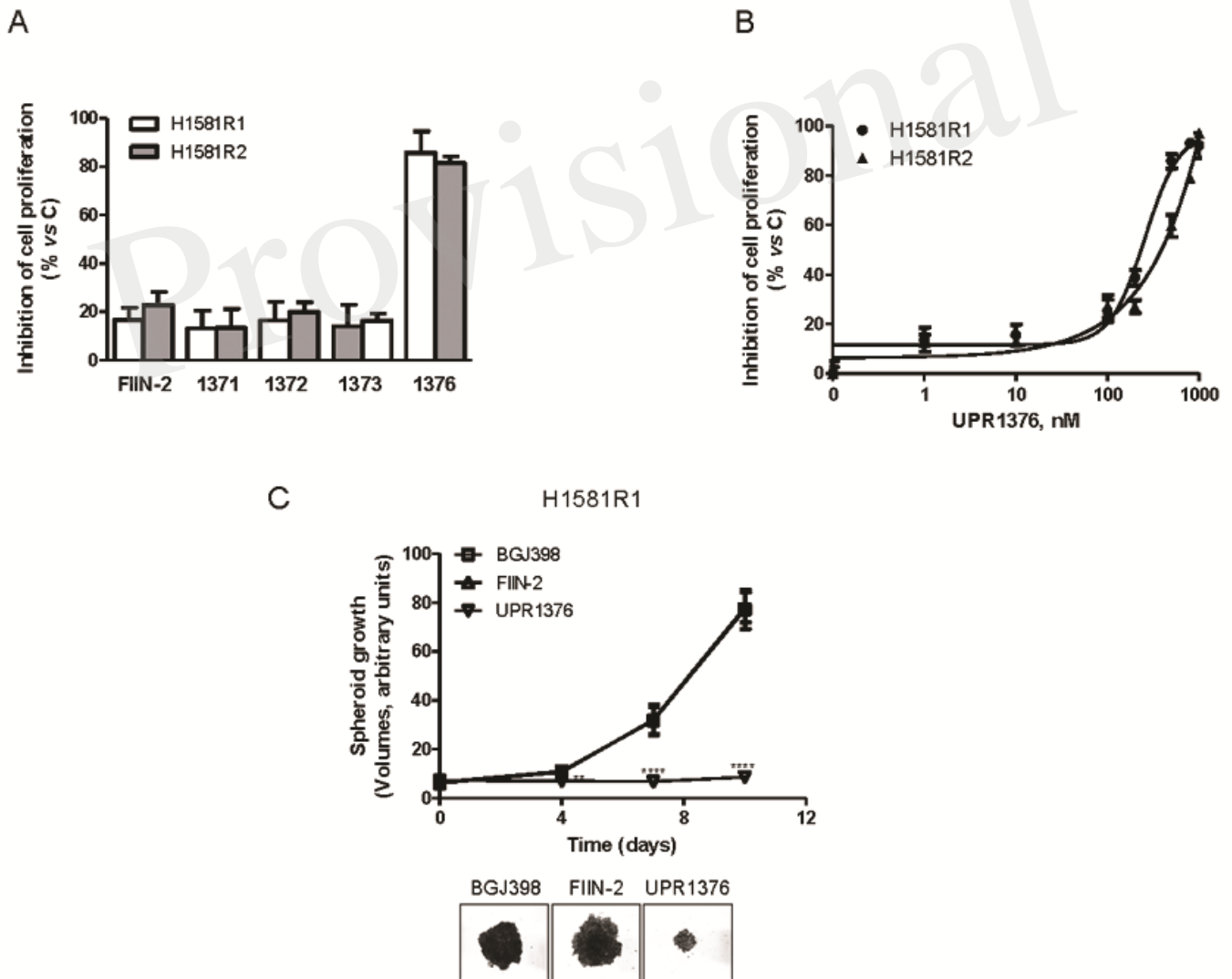


Figure 07.TIF

